

Finite Blocklength Performance of Cooperative Multi-Terminal Wireless Industrial Networks

Yulin Hu, Martin Serror, Klaus Wehrle, and James Gross

Abstract—Cooperative diversity is one of the candidate solutions for enabling ultra-reliable low latency wireless communications (URLLC) for industrial applications. Even if only a moderate density of terminals is present, it allows in typical scenarios the realization of a high diversity degree. It is furthermore only based on a reorganization of the transmission streams, making it achievable even with relatively simple transceiver structures. On the downside, it relies crucially on the distribution of accurate channel state information while cooperative transmissions naturally consume time. With the current goal of providing latencies in the range of 1ms and below, it is thus open if cooperative systems can scale in terms of the number of terminals and the overhead. In this paper, we study these issues with respect to a finite blocklength error model that accounts for decoding errors arising from “above-average” noise occurrences even when communicating below the Shannon capacity. We show analytically that the overall error performance of cooperative wireless systems is convex in the decoding error probability of finite blocklength error models. We then turn to numerical evaluations, where several design characteristics of low latency systems are identified: (I) The major performance improvement is associated with two-hop transmissions in comparison to direct transmissions. The additional improvement due to more hops is only marginal. (II) With an increasing system load, cooperative systems feature a higher diversity gain, which leads to a significant performance improvement despite the increased overhead and a fixed overall frame duration. (III) When considering a realistic propagation environment for industrial deployments, cooperative systems can be shown to generally achieve URLLC requirements.

Index Terms—Finite blocklength, packet error rate, multi-terminal, wireless industrial network, URLLC.

I. INTRODUCTION

THE proliferation of Machine-to-Machine communications in home, business and industrial environments entails new requirements towards wireless communications. Besides optimizing spectral efficiency, future wireless communication standards, such as 5G, will support low latency communication at predictable ultra-high reliabilities [1]. In industrial automation, for example, safety- and mission-critical applications have stringent requirements regarding Quality-of-Service (QoS), which are currently not met by existing wireless standards [2]. Anticipated targets for reliability and latency are typically around $1 - 10^{-9}$ packet delivery ratio (PDR) and 1 ms, respectively [3]. Thus, efficient ways are of interest to increase the communication reliability of wireless networks while achieving low latencies at the same time.

In order to reach the reliability goals, it is clear that diversity either in frequency and/or space need to be exploited, while

exploiting time diversity contradicts the latency requirements. [4] showed that when operating on very short time scales, spatial diversity is especially beneficial for increasing the communication reliability. Moreover, cooperative diversity, a special form of spatial diversity, allows leveraging distributed resources of overhearing terminals. This is particularly useful when the considered terminals have hardware constraints, e. g., when they are limited to a single transceiver antenna for instance due to cost reasons. Then, it is known that cooperative diversity, e. g., cooperative Automatic Repeat reQuest (ARQ), reduces the outage probability by several orders of magnitude [5]. Laneman et al. [5] show that full diversity order in the number of cooperating terminals can be achieved. In [6], [7], a simple scheme is proposed for selecting the “best” relay out of several potential relays based on end-to-end instantaneous Channel State Information (CSI). It is shown that this approach achieves the same performance as more complex space-time coding. The authors of [8] investigate the impact on the transmission delay when using relaying compared to direct transmissions, i. e., under which conditions relaying improves the end-to-end transmission delay. In [9], the authors address ultra-reliable low latency communications (URLLC) networks by proposing a cooperative approach in which nodes simultaneously relay messages to reduce the outage probability. The results show that the transmission reliability increases with the number of participating nodes, even for very low cycle times of 2 ms. Likewise, in [10] a wireless real-time protocol is presented that can achieve latencies within a few milliseconds while providing extremely high reliabilities through cooperative ARQ. Comparably, we showed in previous work [11] that cooperative ARQ can be effectively integrated into a multi-terminal Time Division Multiple Access (TDMA) system with a stringent time deadline.

However, typically these studies are based on idealistic assumptions: (I) Ignoring the overhead for acquiring CSI; (II) Considering arbitrarily reliable communication at Shannon’s channel capacity. Both of these assumptions are too optimistic, especially with respect to URLLC networks. Wireless networks are likely to be comprised of multiple terminals with a significant number of links between the terminals. Hence, the overhead of acquiring CSI is considerable and increases with each additional terminal. Moreover, this increasing overhead reduces the amount of time available for payload transmission. However, in industrial wireless networks, strict latency requirements need to be kept. Effectively, this leads to communication over shorter and shorter blocklengths, which is well known for its significantly different error behavior in comparison to the Shannon outage capacity [12]. In our own previous work, we had studied a *single-terminal* relaying network

operating with finite blocklength codes while the focus is on optimizing/analyzing the throughput performance [13]–[16]. Nevertheless, these results do not carry over to the case of *multi-terminal* URLLC networks. To the best of our knowledge, the reliability performance of such networks leveraging *multi-terminal* cooperative diversity has not been addressed in the finite blocklength regime so far. In multi-terminal systems, the transmission resources are shared and instantaneous CSI must be acquired for each additional link, while on the other hand a larger number of terminals leads in general to a higher diversity degree. To date, the understanding of the trade-off (CSI acquisition cost vs. diversity) is open while it is important to be considered for an efficient system design.

In this work, we investigate these trade-offs with a particular focus on including the overhead as well as basing the system modeling on finite blocklength error models. A growing number of participants in a cooperative multi-terminal network¹ potentially increases the diversity degree while the blocklengths for the individual transmissions decrease. Moreover, as more links must be considered for the relaying paths, the overhead for the collection of CSI increases as well, which additionally reduces the available transmission blocklengths. The fundamental questions addressed in this paper thus are: How reliable can such a wireless network get at a given (low) target latency? Which design decisions should be considered to achieve the anticipated reliability?

Under the consideration of CSI acquisition overhead, and in particular the error model for communication at finite blocklengths, we provide the following core contributions:

- We characterize the error performance of cooperative multi-terminal wireless systems under the Finite Blocklength (FBL) regime. We show in particular that the error performance of a single, tracked terminal, as well as the overall multi-terminal error performance, is convex in the decoding error probability with which the individual links are operated. This is a key result for allowing an efficient optimization of these systems.
- We show numerically that for practical systems at most two hops provide already the largest reliability improvement, when comparing to direct transmission systems. Beyond two hops, the reliability increase is marginal.
- For the case of two-hop relaying, we provide a comparison of two cooperative systems. It is shown that as the cooperative diversity degree increases with an increasing number of terminals in the system, the overall error performance improves *despite* accounting for the overhead and the FBL effects. Furthermore, utilizing Shannon’s outage capacity results can lead to wrong system conclusions with respect to this trade-off.
- Finally, for a realistic propagation environment of a manufacturing scenario, we show that cooperative systems can indeed provide ultra-reliable communications at low latencies despite the necessity to collect instantaneous CSI and utilizing relays, which consumes additional time.

¹The cooperative multi-terminal network we discuss in this work is actually a subcategory of cooperative communication, which can be also called cooperative relaying.

The remainder of this paper is structured as follows. The system model assumptions are presented in Sec. II. In Sec. III, we derive the Packet Error Rate (PER) under the FBL regime; the key performance indicator of the considered system. In Sec. IV, we discuss the PER in the Infinite Blocklength (IBL) regime, this will serve as a reference for the effects of short blocklengths on the system performance. A validation and numerical evaluation of the introduced models is included in Sec. V. A conclusion of this paper is provided in Sec. VI.

II. SYSTEM MODEL AND PROBLEM STATEMENT

We consider a wireless network for URLLC in an industrial context. The network consists of an Access Point (AP) and N associated terminals, which are all in communication range of each other. Time is split into frames of duration T_F . The considered transmission medium is assumed to be a flat radio channel, operating over a given bandwidth B . Transmissions are mainly affected by fading, which we model by a Rayleigh-distributed block-fading process, i.e., channels are static during each frame but vary independently from frame to frame. The instantaneous quality of a link is characterized by the Signal to Noise Ratio (SNR). We denote by $\gamma_{i,j}$ the instantaneous SNR of the link from terminal i to j with $i, j = 0, 1, \dots, N \wedge i \neq j$, where $i = 0$ or $j = 0$ indicates the link from or to the AP. We assume all links to be reciprocal, i.e., $\gamma_{i,j} = \gamma_{j,i}$. Correspondingly, $\bar{\gamma}_{i,j}$ denotes the average SNR and we assume for all links that the average SNR stays constant, i.e., terminals are not mobile. Due to the varying nature of the fading component of the wireless channel, $\gamma_{i,j}$ still varies over time with mean $\bar{\gamma}_{i,j}$. In particular, $\gamma_{i,j} = z\bar{\gamma}_{i,j}$, where z is the channel fading gain which is exponentially distributed with Probability Density Function (PDF):

$$f_Z(z) = \exp(-z) . \quad (1)$$

In general, terminals as well as the access point might have multiple transmit antennas. In those cases, we assume that the average SNR of the links between the antennas of a terminal i and the ones of another terminal j are homogeneous and given by $\bar{\gamma}_{i,j}$. In addition, random channel fading processes across different antennas and different terminals are assumed to be statistically independent.

A central requirement of the system is to ensure high transmission reliability within a fixed latency bound, as industrial applications have stringent delay requirements. Furthermore, in accordance with the considered industrial scenario, we assume that the terminal application generates a *periodic* traffic load, e. g., a proximity sensor that periodically reports the measured distance to a controller. Therefore, a guaranteed medium access needs to be employed, and we consider in the following a TDMA system where the AP centrally assigns time slots to the associated terminals. For each of the N associated terminals, the AP has to guarantee a reliable transmission by fulfilling a target average PER for packets with a given size D (in bits). We assume that the frame time of the TDMA system is set to the periodicity of the data packets, i.e., each terminal holds one packet upon each upcoming transmission frame, where the destination of that packet is some arbitrary

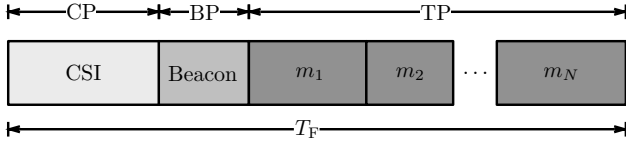


Fig. 1. General structure of the envisioned TDMA frame: The frame starts with a CSI Acquisition Period (CP). Based on this information follows a Beacon Period (BP), which contains the transmission schedule. Note that although we assume a fixed transmission order, the slot lengths and the relay decisions might change from frame to frame. Finally, in the Transmission Period (TP), the N terminals transmit, one after another, their packets.

terminal or the AP within the considered network. In order to increase the reliability the system can employ cooperative transmission, i.e., a packet from a Transmitting Terminal (Tx) to a Receiving Terminal (Rx) may be either transmitted directly or it is relayed via cooperating terminals depending on the link conditions. Thus, to minimize the instantaneous packet error probability, a transmission path between Tx and Rx needs to be selected that provides the highest reliability. However, still all N transmissions need to be accommodated within the frame time T_F . The selection of the best path can be based on instantaneous CSI of all links, which is collected by the AP periodically.

The considered TDMA frame is depicted in Fig. 1. It consists of a CSI Acquisition Period (CP), a Beacon Period (BP), and a Transmission Period (TP). In the CP, the terminals estimate the CSI of all relevant links in the network and report afterwards this information to the AP. Details on the cost of acquiring this CSI are provided in Sec. II-B. In the BP, the AP sends a beacon, which includes a transmission schedule and serves as a synchronization reference for the associated terminals. The TP has a fixed total length of S symbols. It is further divided into N slots with arbitrary blocklengths, each reserved for one of the associated terminals and determined by the scheduler. Each slot length depends on the considered link qualities and on whether a direct or cooperative path was selected by the AP. Regarding the mode of cooperation, during the scheduling process the AP determines for each Tx-Rx pair the best multi-hop path of maximal hop-count W . Note that we do not consider the application of maximum ratio combining or automatic repeat request schemes to be in place in case of the cooperative transmission. The scheduling decision is solely based on the amount of symbols it costs to transmit the packet from Tx to Rx, either by direct transmission, a one-hop cooperative transmission etc. up to W hops. We provide more details on the scheduling process in Sec. II-C.

A. Error Model

A key component impacting any wireless system evaluation is the error model. A commonly used outage performance model is based on the Shannon-Hartley theorem and we refer to this as Infinite Blocklength (IBL) modeling regime. According to the Shannon-Hartley theorem, the capacity function of a complex channel with SNR γ is given by $C_{\text{IBL}}(\gamma) = \log_2(1 + \gamma)$ in bits per channel use. Following the theorem, a transmission from Tx to Rx is error-free if $C_{\text{IBL}}(\gamma) = \log(1 + \gamma) \geq r \Leftrightarrow \gamma \geq 2^r - 1$, where r denotes the coding rate (bit/channel

use). If this requirement is not fulfilled, the packet cannot be decoded correctly, which leads to a packet *outage*. The probability of the outage occurring in an instantaneous single-hop transmission is denoted by

$$p_{\text{out}} = \mathbb{P}\{\gamma < 2^r - 1\}. \quad (2)$$

When assuming perfect CSI at the Tx, i.e., the instantaneous γ is known, an appropriate rate r can be determined such that p_{out} gets zero. To transmit a packet with size D , different values of coding rate r lead to different costs of transmitting symbols, i.e., the symbol cost (blocklength) results as

$$M \geq D/r \geq D/C_{\text{IBL}}(\gamma). \quad (3)$$

In other words, under the IBL regime a successful transmission of a packet costs a random number of symbols due to the random channel fading. As a result, when imposing a limited duration of the frame T_F , which can be interpreted as a deadline, the timing/symbol budget might not suffice to reliably convey the packet, or in the multi-user context all packets. Thus, a packet error occurs and we refer to this error type as *scheduling error*.

However, it is well known that the Shannon-Hartley theorem becomes less accurate for systems with short blocklengths, i.e., packet transmissions over only a limited number of symbols, as is the case in our study. This is due to the fact that it assumes coding blocks of arbitrary length such that the temporarily varying noise averages out. While for several thousands of symbols per frame this assumption is more or less justified, for low latency systems it is clearly not the case. This motivates us to consider a second error model, which we refer to as Finite Blocklength (FBL) modeling regime. In this case, for the real Additive White Gaussian Noise (AWGN) channel, [12] derives an accurate approximation of the coding rate for a direct transmission under the finite blocklength assumption. With a given blocklength M , SNR γ , and coding rate r , the error probability ε is given by

$$\varepsilon \approx Q\left(\frac{\frac{1}{2}\log_2(1 + \gamma) - r}{\sqrt{V_{\text{real}}/M}}\right), \quad (4)$$

where $Q(w) = \int_w^\infty \frac{1}{\sqrt{2\pi}} e^{-t^2/2} dt$ is the Gaussian Q-function. In addition, V_{real} is the channel dispersion of a real Gaussian channel given by $V_{\text{real}} = \frac{\gamma}{2} \frac{\gamma+2}{(1+\gamma)^2} (\log_2 e)^2$. This result has been extended to complex quasi-static fading channel models [17]–[21]. For a direct transmission under a quasi-static fading channel and with perfect CSI at the Tx, the decoding error probability at the Rx is

$$\varepsilon \approx Q\left(\frac{C_{\text{IBL}}(\gamma) - r}{\sqrt{V_{\text{comp}}/M}}\right), \quad (5)$$

where the channel dispersion of a complex Gaussian channel is $V_{\text{comp}} = 2V_{\text{real}}$. These approximations have been shown to be tight for sufficiently large values of M [12], [22]. In the remainder of the paper, we consider sufficiently large values of M meaning that we assume Eq. (5) to hold with equality.

Comparing Eq. (2) with Eq. (5), the difference between the two error models becomes evident: Errors under the IBL regime are solely caused by scheduling, i.e., not enough

symbols being available to schedule the fixed-size packet with the appropriate coding rate. However, the error probability under the FBL regime results from scheduling errors on the one hand, while in addition also *decoding errors* at the receiver might occur due to above-average noise incidents.

B. Overhead Model for CSI Collection and Scheduling

We introduce an overhead model for the CSI acquisition period at the beginning of the TDMA frame as well as the beacon transmission to announce the scheduling decisions, cf. Fig. 1. In particular, we are interested in quantifying the amount of symbols that this acquisition consumes, which reduces subsequently the amount of symbols available for the payload transmission. Recall that the AP relies on instantaneous CSI to schedule the transmissions. Thus, we assume that during the CP, the current link conditions for each link must first be determined and subsequently communicated to the AP. This introduces two types of overhead, namely *estimation* overhead and *communication* overhead, i.e., the former corresponds to the cost of sending a reference signal for each Tx-Rx pair, while the latter is spent for transmitting the collected CSI to the AP. Once the AP has received all CSI, it determines the schedule and indicates it to the terminals through the beacon. The beacon contains apart from the selected path also the timing information, i.e., when which terminal starts packet transmissions either as source or as relay in a cooperative path. We refer to the cost of transmitting a beacon in a frame as *signaling* overhead.

We assume reciprocal link qualities such that incoming and outgoing links do not need to be considered separately. All links from and to the AP can thus be directly estimated by the AP, leading to no communication overhead for these links, while the estimation overhead for these links remains. Furthermore, we assume a fixed order for estimating the link qualities and reporting them to the AP, i.e., each terminal, one after the other, sends a reference signal. Afterwards, in the same order, the terminals report their measurements to the AP. For a single link, we define S_e as the duration of the reference signal in symbols, S_c indicates the number of symbols required to represent the link quality accurately, i.e., the communication overhead per link, and S_s is the amount of needed symbols to schedule a single terminal, which influences the signaling overhead. Note that N terminals are required to be served in each frame. Then, the total number of symbols to estimate the qualities of all links is given by $N \cdot S_e$. For the communication overhead, note that any terminal including the AP may potentially act as relay, leading to a fully connected network, while links from and to the AP can be excluded. Hence, the total number of considered links is $\frac{N(N-1)}{2}$ and the corresponding overhead is $\frac{(N-1)}{2} \cdot S_c$. Furthermore, the total signaling overhead results to $N \cdot W \cdot S_s$, as for a W -hop path W scheduling announcements need to be signaled. Finally, the total overhead in terms of symbols is given by $S_o = N \cdot (S_e + \frac{(N-1)}{2} \cdot S_c + W \cdot S_s)$.

C. Problem Statement

As discussed previously, the AP schedules for each transmission the path with the minimal cost in terms of symbols

consumed. For the transmission originating at terminal i we denote the symbol cost of a direct transmission by $M_{D,i}$ and the minimum symbol cost of cooperative relaying is denoted by $M_{R,i}$. The multi-hop transmission might include w hops with $w \in [2, W]$, and we denote those links by $R_v, v = 1, \dots, w$. Fixing the number of hops to w , the minimum symbol cost over all possible hops is denoted by $M_{R,i,w}$, and we have $M_{R,i,w} = \sum_{v=1}^w M_{R_v,i}$, where $M_{R_v,i}$ is the cost at link R_v . Given this, the minimum symbol cost of all multi-hop paths $M_{R,i}$ is then the minimal one over all possible numbers of relaying hops, i.e., $M_{R,i} = \min_{w \in [2, W]} \{M_{R,i,w}\}$. For each Tx-Rx pair to be served during the frame we assume the AP determines the optimal path through solving a shortest-path routing problem where the symbol costs represent the weights of the edges of a corresponding graph. Therefore, the AP selects the path option with the minimal cost, i.e., $M_{\min,i} = \min\{M_{R,i}, M_{D,i}\} = \min_{w \in [2, W]} \{M_{R,i,w}, M_{D,i}\}$. The AP tries to schedule all N terminals based on a fixed transmission order. Aggregating all terminal transmissions, it is possible that due to the fading the number of symbols S of the data transmission phase of the frame does not suffice to reliably convey all N packets. In this case, the first packets are scheduled until the frame length of S symbols is exceeded and the remaining packets are dropped, leading to *scheduling errors*. Let us denote the probability that the first i packets are successfully scheduled by p_i , where $p_i = \mathbb{P}\left\{S \geq \sum_{k=1}^i M_{\min,k}\right\}$. Hence, the probability of packet i being dropped due to a scheduling error is given by $1 - p_i$. If scheduling errors were the only source of errors in the system, as is ideally modeled through the IBL assumption, the corresponding system performance would directly follow from the above expressions. Thus, from a system perspective the average PER over N packets results to

$$\text{PER}_{\text{IBL}} = \frac{1}{N} \sum_{i=1}^N \{1 - p_i\} . \quad (6)$$

Nevertheless, in real transmission systems decoding errors might occur in addition, which is captured by the FBL error model. Thus, when scheduling the individual links, the AP needs to consider a target decoding error probability ε^* when allocating the symbols for each packet transmission, which is either direct or multi-hop. This target error probability influences the overall reliability of an individual transmission and of the entire system. Let us denote the choice of target error probability in the scheduling process of the AP by ε^* .² Assuming that the AP chooses a path with w hops, the corresponding overall Tx-Rx error probability results to $1 - (1 - \varepsilon^*)^w \approx w\varepsilon^*$.³ Factoring in the likelihood of choosing the direct link versus the w -hop cooperative paths, the average probability of losing a packet for terminal i is denoted by $\varepsilon_{\text{ave},i}$. Thus, the expected error probability for a scheduled packet i is $\varepsilon_{\text{ave},i}^* = \mathbb{P}\{M_{D,i} \text{ is lowest cost}\} \cdot \varepsilon^* +$

²Note that we do not consider individual target error probabilities for each terminal i in the following.

³Considering reliable wireless systems with $\varepsilon^* \ll 10^{-1}$, thus, we have $1 - (1 - \varepsilon^*)^2 \approx 2\varepsilon^* - (\varepsilon^*)^2 \approx 2\varepsilon^*$, $1 - (1 - \varepsilon^*)^3 \approx 3\varepsilon^* - 3(\varepsilon^*)^2 + (\varepsilon^*)^3 \approx 3\varepsilon^*$, and similar for cases with $w \geq 4$.

$\sum_{w=2}^W \mathbb{P}\{M_{R,i,w} \text{ is lowest cost}\} \cdot w\varepsilon^*$. This finally results in the combined PER of a packet i under the FBL regime

$$\text{PER}_{\text{FBL},i} = 1 - p_i + p_i \cdot \varepsilon_{\text{ave},i}^*, \quad (7)$$

which results in the overall error probability of the entire system as

$$\begin{aligned} \text{PER}_{\text{FBL}} &= \frac{1}{N} \sum_{i=1}^N \text{PER}_{\text{FBL},i} \\ &= \frac{1}{N} \sum_{i=1}^N \{1 - p_i + p_i \varepsilon_{\text{ave},i}^*\}. \end{aligned} \quad (8)$$

The probabilities of scheduling errors and decoding errors are related through the choice of ε^* . If ε^* is chosen large, a larger coding rate follows which leads to a smaller scheduling cost $M_{\min,i}$ per terminal i and therefore decreases the scheduling error probability $1 - p_i$. However, this increases obviously the average decoding error probability $\varepsilon_{\text{ave},i}^*$. In contrary, lowering the choice of ε^* lowers the average decoding error probability $\varepsilon_{\text{ave},i}^*$ at the cost of a larger scheduling error probability $1 - p_i$, as the coding rate needs to be decreased, leading to a larger scheduling cost $M_{\min,i}$ per terminal i . In the following, we are interested in characterizing the optimal trade-off between these two effects. In order to study this trade-off, however, first a more detailed model needs to be derived. Given this model for the PER performance, we are interested in the following fundamental questions: (I) What is the optimal choice of ε^* with respect to the overall PER performance? (II) What is the impact of system aspects such as the overhead for CSI acquisition and for beacon transmissions on the overall system performance? How do these effects impact the optimal choice of ε^* ? (III) How is the system performance affected when analyzing the considered cooperative system under the IBL regime instead of the FBL regime? How important is it to take the decoding errors into account and by how much is the real system performance overestimated when modeling the PER only via the IBL regime?

III. PACKET ERROR PROBABILITY IN THE FINITE BLOCKLENGTH REGIME

The receiver SNRs are random variables subject to channel fading. The cost of reliably transmitting a packet from a terminal i to a terminal k , in terms of symbols, thus varies over time along with the random channel fading. We characterize this random cost by the PDF $f_{M_{i,k}}(m)$. Consequently, the PDFs of $M_{\min,i}$, $M_{D,i}$, and $M_{R,i,w}$ (cf. Sec. II-C) are denoted by $f_{M_{\min,i}}(m)$, $f_{M_{D,i}}(m)$, and $f_{M_{R,i,w}}(m)$, respectively. In the following, we first focus on $f_{M_{\min,i}}(m)$ and on the average PER (over the channel fading) of the considered system for given PDFs $f_{M_{R,i,w}}(m)$ and $f_{M_{D,i}}(m)$, $i = 0, \dots, N$. Then, we turn to the derivation of the Cumulative Distribution Functions (CDFs) $F_{M_{R,i,w}}(m)$ and $F_{M_{D,i}}(m)$ for the considered multi-hop system. This allows us then to consider the impact of the target error probability ε^* under the FBL regime on the overall error probability of the system, which is the main contribution of this paper.

A. Average PER

Recall that $M_{D,i}$ and $M_{R,i}$ are the minimum symbol costs for transmitting the packet for terminal i via direct transmission and multi-hop relaying with up to W hops. In addition, $M_{R,i,w}$ is the minimum cost for conveying the packet over a w -hop path. Let us assume that the CDFs of $M_{D,i}$, $M_{R,i}$ and $M_{R,i,w}$ are given by $F_{M_{D,i}}(m)$, $F_{M_{R,i}}(m)$ and $F_{M_{R,i,w}}(m)$, respectively. Hence we have

$$F_{M_{R,i}}(m) = 1 - \prod_{w=2}^W (1 - F_{M_{R,i,w}}(m)). \quad (9)$$

We denote by $M_{\min,i}$ the minimal cost between direct transmission and relaying and by $F_{M_{\min,i}}(m)$ the CDF of $M_{\min,i}$. Then, $1 - F_{M_{\min,i}}(m)$ indicates the probability of $m > M_{\min,i}$, which further equals the probability $(1 - F_{M_{D,i}}(m))(1 - F_{M_{R,i}}(m))$, i.e., the probability of m being larger than both $M_{D,i}$ and $M_{R,i}$. Therefore, $F_{M_{\min,i}}(m)$ can be derived as follows

$$\begin{aligned} F_{M_{\min,i}}(m) &= 1 - (1 - F_{M_{D,i}}(m))(1 - F_{M_{R,i}}(m)) \\ &= 1 - (1 - F_{M_{D,i}}(m)) \prod_{w=2}^W (1 - F_{M_{R,i,w}}(m)). \end{aligned} \quad (10)$$

Hence, the PDF of $M_{\min,i}$ is given by

$$\begin{aligned} f_{M_{\min,i}}(m) &= f_{M_{D,i}}(m) \prod_{w=2}^W (1 - F_{M_{R,i,w}}(m)) \\ &+ (1 - F_{M_{D,i}}(m)) \sum_{v=2}^W \left\{ f_{M_{R,i,v}}(m) \prod_{v \in [2,W], v \neq w} (1 - F_{M_{R,i,w}}(m)) \right\}. \end{aligned} \quad (11)$$

Based on the CSI, the AP determines the transmission mode for each packet, i.e., either sending it over the best w -hop path or by direct transmission. Recall that in total N packets need to be transmitted during a frame while the minimal cost for transmitting a packet from terminal i is $M_{\min,i}$, $i = 1, \dots, N$. Note that $M_{\min,i}$, $i = 1, \dots, N$, are approximately i.i.d., especially for networks with larger numbers of terminals⁴. Then, the PDF of the sum of the costs of transmitting all N packets $M_{\text{sum},N} = \sum_{i=1}^N M_{\min,i}$ is given based on Eq. (11) as

$$f_{M_{\text{sum},N}}(m) = f_{M_{\min,1}}(m) \otimes \dots \otimes f_{M_{\min,N}}(m), \quad (12)$$

where \otimes is the convolution function. The cost of transmitting the first n packets is given by $M_{\text{sum},n} = \sum_{i=1}^n M_{\min,i}$. Thus, the probability that the first n packets are successfully transmitted in a frame with total blocklength S is given by

$$p_n = F_{M_{\text{sum},n}}(S). \quad (13)$$

To derive the average PER over all N packets, denoted by PER_{FBL} , the target error probability ε^* needs to be considered. For a scheduled packet of terminal i ,

⁴In Sec. V, we validate the appropriateness of this approximation by simulation.

if the transmission is performed directly, which happens with probability $\mathbb{P}\left\{\min_{w \in [2, W]} \{M_{R,i,w}\} \geq M_{D,i}\right\} = \sum_{m=1}^{+\infty} F_{M_{D,i}}(m) f_{M_{R,i}}(m)$, the decoding error probability is ε^* , as only a single link is involved. In addition, according to (9), $f_{M_{R,i}}(m)$ is given by $f_{M_{R,i}}(m) = \sum_{v=2}^W [f_{M_{R,i,v}}(m) \prod_{w \in [2, W], w \neq v} (1 - F_{M_{R,i,w}}(m))]$. On the other hand, if a w -hop path is more efficient, which happens with probability $\mathbb{P}\left\{\min_{v \in [2, W]} \{M_{R,i,v}\} = M_{R,i,w} < M_{D,i}\right\} = \sum_{m=1}^{+\infty} \left\{f_{M_{R,i,w}}(m) [1 - F_{M_{D,i}}(m)] \prod_{\substack{v \neq w \\ v \in [2, W]}} (1 - F_{M_{R,i,v}}(m))\right\}$, the transmission of the packet from terminal i has a decoding error probability $w \cdot \varepsilon^*$. Marginalizing over the options for the different paths of length w , the expected decoding error probability for packet i is given by

$$\varepsilon_{\text{ave},i}^* = \varepsilon^* \sum_{m=1}^{+\infty} F_{M_{D,i}}(m) f_{M_{R,i,w}}(m) + \sum_{w=2}^W w \varepsilon^* \sum_{m=1}^{+\infty} \left\{f_{M_{R,i,w}}(m) [1 - F_{M_{D,i}}(m)] \prod_{\substack{v \neq w \\ v \in [2, W]}} (1 - F_{M_{R,i,v}}(m))\right\}. \quad (14)$$

The combined PER for the i th packet and the average PER over all N packets follows then from Equations (7) and (8).

B. Distribution of the Transmission Blocklengths

According to Eq. (5), the error probability of a single-hop transmission with packet size D and blocklength M is

$$\varepsilon = Q \left(\frac{C_{\text{IBL}}(\gamma) - D/M}{\log_2 e \sqrt{(1 - (1 + \gamma)^{-2})/M}} \right). \quad (15)$$

Let us assume in the following that the decoding error probability of each transmission is required to be lower than 0.5. Then the minimal blocklength M^* satisfies

$$\varepsilon^* = Q \left(\frac{C_{\text{IBL}}(\gamma) - D/M^*}{\log_2 e \sqrt{(1 - \frac{1}{(1+\gamma)^2})/M^*}} \right). \quad (16)$$

In particular, we further have

$$\left(\sqrt{M^*}\right)^2 - \lambda \sqrt{M^*} - D/C_{\text{IBL}}(\gamma) = 0, \quad (17)$$

where $\lambda = Q^{-1}(\varepsilon^*) \frac{\log_2 e \sqrt{(1 - \frac{1}{(1+\gamma)^2})}}{C_{\text{IBL}}(\gamma)}$, which leads to

$$\sqrt{M^*} = \sqrt{\frac{D}{C_{\text{IBL}}(\gamma)} + \left(\frac{\lambda}{2}\right)^2} + \frac{\lambda}{2}. \quad (18)$$

Finally, this results in a minimal blocklength M^* of

$$M^* = \frac{D}{C_{\text{IBL}}(\gamma)} + \frac{1}{2} \lambda^2 + \lambda \sqrt{\frac{D}{C_{\text{IBL}}(\gamma)} + \left(\frac{\lambda}{2}\right)^2}. \quad (19)$$

Obviously, M^* is a function of γ and λ , while λ is a function of γ . Consequently, M^* is a function of γ . We denote this function as $g(\cdot)$, i. e., $M^* = g(\gamma)$. Then, the corresponding inverse function is given by $\gamma = g^{-1}(M^*)$. Based on the channel gain distribution in Eq. (1), the CDF of M^* is

$$F_{M^*}(m, \bar{\gamma}) = \int_{z \in \Omega} f_Z(z) dz = \int_0^{\frac{g^{-1}(m)}{\bar{\gamma}}} f_Z(z) dz, \quad (20)$$

where $\Omega = \{z : M^*(z\bar{\gamma}) \leq m\}$. Then the PDF of M^* of a single-hop link with average channel gain $\bar{\gamma}$ is

$$f_{M^*}(m, \bar{\gamma}) = \frac{\partial F_{M^*}(m)}{\partial m} = \frac{p\left(\frac{g^{-1}(m)}{\bar{\gamma}}\right)}{\bar{\gamma} \frac{\partial g(g^{-1}(m))}{\partial m}}. \quad (21)$$

In general, the blocklength should be a non-negative integer, while the above model is based on a continuous random variable m . It should be mentioned that in this work we consider sufficiently large values of blocklength, i. e., $f_{M^*}(m, \bar{\gamma}) \approx f_{M^*}(m + t, \bar{\gamma})$, $t \in [0, 1)$. For simplicity, we obtain the PDF of the discrete random variable m by sampling the above continuous model, which results in the PDF $f_{M^*}(m, \bar{\gamma})$, $m = 0, 1, 2, \dots, +\infty$. In addition, we will validate this approximation by means of simulations in Sec. V-B.

Then, the PDF of the cost of transmitting a packet via the direct link between terminal i and k can be expressed as $f_{M_{D,i}}(m) = f_{M^*}(m, \bar{\gamma}_{i,k})$. For a w -hop relaying transmission, Eq. (21) can be applied for each hop and thus the PDF of the total cost over w hops is a product convolution:

$$f_{M_{R,i,w}}(m) = f_{M_{R_1,i}}(m) \otimes f_{M_{R_2,i}}(m) \otimes \dots \otimes f_{M_{R_w,i}}(m), \quad (22)$$

where $f_{M_{R_v,i}}(m) = f_{M^*}(m, \bar{\gamma}_{v,i})$, $v = 1, \dots, w$, is the PDF of the cost at v -th hop for transmitting packet i and $\bar{\gamma}_{v,i}$ is the average SNR of this hop.

By applying the above PDFs of $M_{D,i}$, $M_{R,i,w}$ and $M_{\min,i}$ to (8) and (14), the PER model of the considered system can be obtained. We are now in the position to state the main result of our work, namely that the overall packet error rate is a convex function of the choice of target decoding error probability ε^* , and thus we can optimize the overall average packet error rate or also the one per terminal based on this result. This captures essentially the trade-off between scheduling errors and decoding errors under the FBL regime. We have the following proposition.

Proposition 1: For the FBL regime and for the considered cooperative system, the average PER of a single packet i , denoted by $\text{PER}_{\text{FBL},i}$ with $i = 1, \dots, N$ as well as the average system PER over all N packets transmitted per frame, denoted by PER_{FBL} , are both convex in the target decoding error probability ε^* .

Proof: See Appendix A. ■

According to Proposition 1, the reliability of the whole network can be efficiently optimized by applying convex optimization techniques to determine the optimal target error probability for transmitting a single packet. Note that in a system deployment this optimization only has to be run once at the initialization of the system, unless the average SNRs or essential system parameters like the packet size, frame duration, etc. change.

IV. PACKET ERROR PROBABILITY IN THE INFINITE BLOCKLENGTH REGIME

Recall that under the IBL regime, a single-hop transmission is error free if $C_{\text{IBL}}(\gamma) = \log(1 + \gamma) \geq \frac{D}{M} \Leftrightarrow \gamma \geq 2^{\frac{D}{M}} - 1$. Hence, the minimal blocklength cost M^* for successfully transmitting a packet is the realization of a random variable. Considering that it is required to transmit N packets per frame within a fixed frame length of S symbols, the transmission error of the considered system in the IBL regime is fully subject to scheduling, i.e., the sum of the minimal costs for transmitting N packets may be larger than S . Since we assume a block-fading Rayleigh channel, the CDF of the minimal blocklength M^* for transmitting a packet of size D via a single-hop transmission with average SNR $\bar{\gamma}$ is given by

$$\begin{aligned} F_{M^*}(m, \bar{\gamma}) &= \Pr\{M^* \leq m\} = \Pr\{\gamma \geq 2^{\frac{D}{m}} - 1\} \\ &= \exp\left[-\frac{1}{\bar{\gamma}} \left(2^{\frac{D}{m}} - 1\right)\right]. \end{aligned} \quad (23)$$

The PDF of the minimal cost t^* of a single-hop transmission with average SNR $\bar{\gamma}$, assuming that t is a continuous random variable, is then given by

$$f_{t^*}(t, \bar{\gamma}) = \exp\left[-\frac{1}{\bar{\gamma}} \left(2^{\frac{D}{t}} - 1\right)\right] \cdot \frac{2^{\frac{D}{t}}}{\bar{\gamma}} \cdot \frac{D \ln 2}{t^2}. \quad (24)$$

Note that the real cost M (in symbols) is an integral. Hence, we have $M^* = \lceil t^* \rceil$, where $\lceil \cdot \rceil$ is a function that rounds up to the nearest integer. Then, the CDF of the minimal cost in symbols is

$$F_{M^*}(t, \bar{\gamma}) = \int_1^m \exp\left[-\frac{1}{\bar{\gamma}} \left(2^{\frac{D}{t}} - 1\right)\right] \cdot \frac{2^{\frac{D}{t}}}{\bar{\gamma}} \cdot \frac{D \ln 2}{t^2} dt. \quad (25)$$

The average PER over all N packets can be obtained by Eq. (6). Note that the IBL regime can be seen as a special case of the FBL regime, where $m \rightarrow +\infty$ and $\epsilon^* \rightarrow 0$. Hence, the derivations in the previous section still hold in the IBL regime. In particular, we can derive p_i for relaying by substituting Eq. (23) and Eq. (24) in Eq. (22), Eq. (10) and Eq. (8).

V. PERFORMANCE EVALUATION

In this section, we empirically evaluate the finite block-length performance of the considered multi-terminal wireless industrial network. Firstly, we introduce the evaluation methodology and parameterization in Sec. V-A. Secondly, in Sec. V-B, we study the features of the shown convexity of the PER with respect to the target error probability. In particular, we are interested in the behavior of the convexity with different system setups. Thirdly, we move to a more general performance investigation in Sec. V-C and, in particular, analyze the performance gap between FBL and IBL. The evaluation of an industrial automation use-case is presented in Sec. V-D. Finally, we extend our model to Rician fading channels (cf. Sec. V-E) and analyze the throughput performance (cf. Sec. V-F).

TABLE I
VALIDATION/EVALUATION PARAMETERS.

Symbol	Value	Description
B	5 MHz	Channel bandwidth
T_F	1 ms	Frame length in time
S	5000	Total amount of symbols per frame
N	5	Number of transmissions per frame
D	400 bit	Packet size
S_e	8	Symbols for estimating one link
S_c	8	Symbols for collecting quality of one link
S_s	24	Symbols for scheduling one terminal
$\bar{\gamma}$	15 dB	Average SNR at the receiver

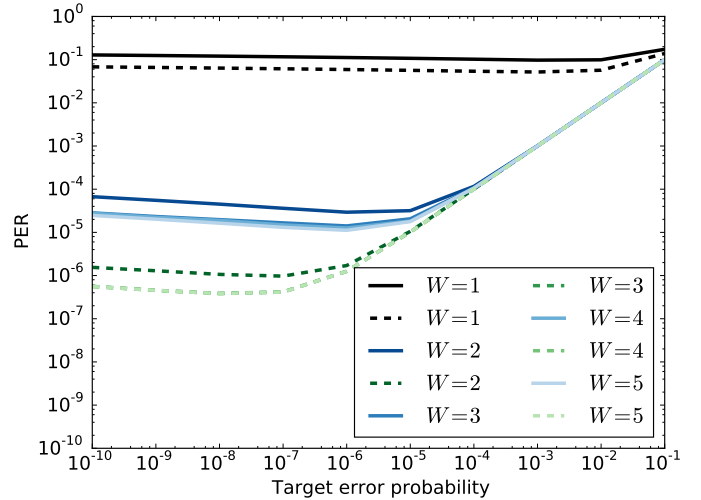


Fig. 2. PER for an increasing number of hops (W) varying the target error probability ϵ^* . For solid lines the avg. link quality is $\bar{\gamma} = 5$ dB, while for dashed lines the avg. link quality is $\bar{\gamma} = 7.5$ dB.

A. Methodology

We start with an evaluation of the proposed system by means of simulations under a parameterization of the system model given in Table I. We are in particular interested initially in the benefit of considering longer and longer paths on the overall error probability. Fig. 2 shows the average packet error rate of the system over an increasing path length (W) considered during the scheduling process, where $W = 1$ represents direct transmissions from Tx to Rx. With $W = 2$, a packet might be relayed via one relay, with $W = 3$, a packet might be relayed via up to two relays and so on. In the simulations, for a given instance the optimal path is always chosen considering the limitation on W though. Note that the scheduling requires more and more computation time if longer path lengths are considered. Fig. 2 initially reveals a significant performance improvement as the system moves from direct transmission to also exploiting multi-hop paths. However, from Fig. 2 we observe that the major performance improvement is reaped off already when considering only 2-hop transmissions in addition to the direct transmissions. Fig. 2 also shows the convex behavior for the packet error rate as a function of the decoding error probability ϵ . For any multi-hop setting, an optimal choice of decoding error probability ϵ exists, which nevertheless is dependent on the system parameters.

Due to the marginal improvement in the packet error probability if more than 2 hops are considered by the scheduler,

we limit in the following the investigations to systems with at most $W = 2$ hops. In particular, we compare the system performance of two specific system variants:

BEST-ANTENNA: This system realizes an asymmetric distribution of hardware resources as it is common in cellular networks, i.e., a complex, powerful base station and less complex terminals. Terminals are typically limited regarding memory, processing capabilities and transmission antennas in comparison to the AP. Therefore, in this system set-up cooperative transmission is solely performed by the AP. Transmissions are thus either directly sent from Tx to Rx or indirectly via the (multi-antenna) AP. For simplicity, we assume that the AP uses antenna selection to pick the currently best link for incoming and outgoing transmissions and possibly different antennas on the incoming and outgoing transmission of the same packet. An example for the relaying in the BEST-ANTENNA system set-up is illustrated in Fig. 3 (a-b). Minor modifications need to be considered with respect to the overhead model. In the case of BEST-ANTENNA, packets are either transmitted directly between Tx and Rx or indirectly via the AP, all relay links can thus be estimated by the AP. Only for direct transmissions, the respective links are estimated by the terminals and consequently this information must be conveyed to the AP. Thus, a total of N links must be characterized, leading to a total overhead of $N \cdot S_c$. Hence, the total overhead per frame in BEST-ANTENNA is $S_o = N \cdot (S_e + S_c + S_s)$. Below, we consider multiple scenarios with different numbers of antennas at the AP for the best antenna selection. To distinguish these BEST-ANTENNA set-ups, we denote by k *Antenna* a scenario with k antennas at the AP.

BEST-RELAY: The second system set-up makes full use of the existing distributed resources, assuming that terminals and AP have (more or less) comparable hardware characteristics. Apart from the direct transmission path for a packet between Tx and Rx, any overhearing terminal in the cell may act as relay to transmit the packet. However, following our findings from above, at most 2-hop paths are realized in the system, i.e., the AP selects for each transmission a direct transmission path or the best available 2-hop path based on instantaneous CSI. An example of the system operation in case of BEST-RELAY is illustrated in Fig. 3 (c-d). With respect to the overhead model, consider that in BEST-RELAY, any terminal including the AP may potentially act as relay, leading to a fully connected network. However, since links from and to the AP can be excluded, the total number of considered links is $\frac{N(N-1)}{2}$. This leads, for BEST-RELAY, to a total overhead in terms of symbols of $S_o = N \cdot (S_e + \frac{(N-1)}{2} \cdot S_c + S_s)$. In the following, we consider multiple scenarios with a different number of relays. We denote by k *Relay* the scenario with k available terminals to act as relay candidates. In particular, when all terminals may act as relay candidate, we call this scenario *Max Relay*.

Quantization Model of the CSI: Our analytical derivations rely on the existence of perfect CSI at the AP. In a practical deployment, however, the quantization of the CSI and its reliable transmission to the AP must be considered. Therefore, before considering more detailed evaluations, we first study the effects of a quantized CSI on the system performance to find

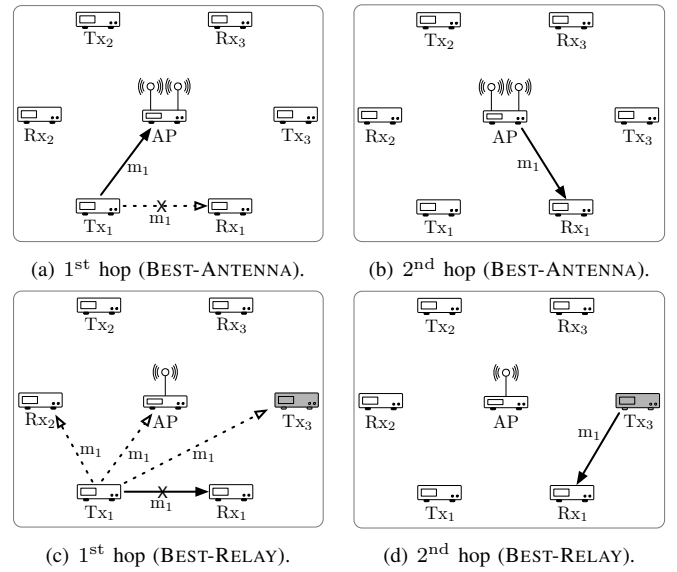


Fig. 3. Example scenario for transmitting a packet m_1 from Tx_1 to Rx_1 , using BEST-ANTENNA (a-b) and BEST-RELAY (c-d). In (a), the AP schedules an indirect transmission of m_1 , as the direct link is currently in a bad state, selecting the currently best antenna to receive m_1 . In (b), m_1 is successfully transmitted from AP to Rx_1 , again using the currently best antenna for transmission. In (c), three distinct relays overhear m_1 , while the direct transmission fails. In (d), m_1 is relayed by Tx_3 , the best available relay.

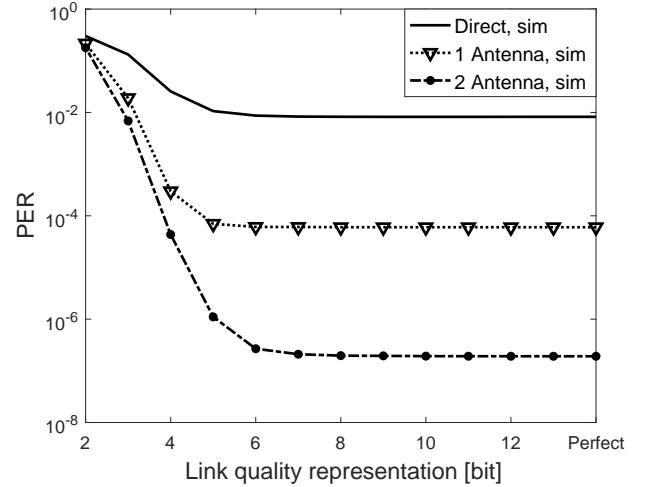


Fig. 4. PER depending on the quantization of link qualities. We vary the number of bits used to represent a single link quality, where *perfect* is the reference for an arbitrarily high representation.

the right trade-off for the overhead cost. As a reference, we use a simple uniform quantizer for the channel states, which we define as follows

$$U(\gamma) = \Delta \cdot \left\lceil \frac{\gamma}{\Delta} + 0.5 \right\rceil, \quad (26)$$

where Δ denotes the step size depending on the number of bits used to represent the quality of a single link. We simulate DIRECT (no cooperative diversity) and BEST-ANTENNA and consider a varying number of bits used to represent the CSI. For each data point, we generate at least 10^8 transmission frames to be able to empirically observe the expected PER. The results are shown in Fig. 4. We see that, in general, when increasing the cooperative diversity in the system, i.e.,

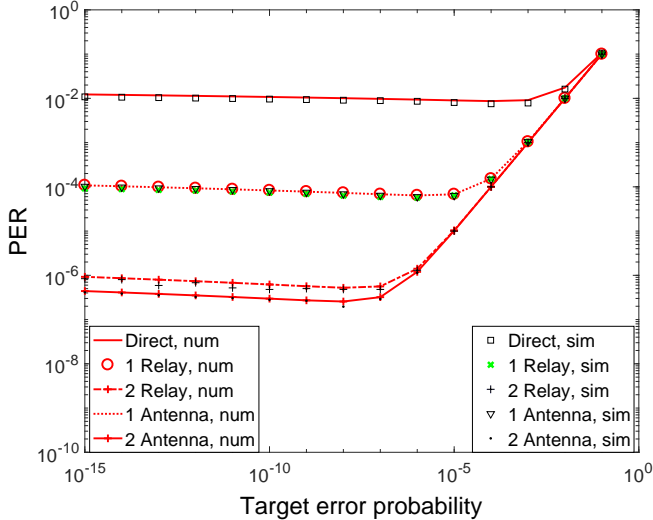


Fig. 5. Simulative validation of the analytical models for DIRECT, BEST-RELAY, and BEST-ANTENNA under the FBL regime varying the target error probability ϵ^* .

shifting from DIRECT to 2 Antenna, the PER decreases by several orders of magnitude. When moving from a perfect representation of the link quality to a quantized representation, the PER remains relatively stable until a certain representation, e.g., 6 bit for BEST-ANTENNA. Below this point, the PER strongly increases. We thus set the overhead $S_c = 8$ for our evaluation, allowing at least 8 bit to be reserved for the quality representation of one link. The remaining overhead parameters are adapted accordingly. With this overhead parameterization, in the following we assume that the quantized CSI has a negligible influence on the PER.

B. Convexity of the PER

We empirically validate PER_{FBL} (cf. Eq. (8)) depending on ϵ^* for DIRECT, BEST-RELAY, and BEST-ANTENNA by simulations. For this, we consider a rather synthetic scenario where all links have the same average SNR $\bar{\gamma} = 15$ dB. Given this scenario and the parameterization as shown in Table I, we generate random instances of the receiver SNR, which are used to calculate, for each transmission, the minimal blocklength M^* and subsequently to compute the respective PER. For BEST-RELAY and BEST-ANTENNA, we set the number of available relays/antennas to one and two, leading to PERs that can be verified by simulations in a reasonable amount of time.

The respective results are depicted in Fig. 5. Markers indicate simulation results, while lines indicate the respective numerical results for comparison. We observe that the simulation accurately matches the numerical results as only small deviations are observed due to a finite number of samples in the simulation. This indicates that our approximation of $2\epsilon^* + (\epsilon^*)^2$ by $(\epsilon^*)^2$ is appropriate even for cases when the PER is up to 10^{-1} . In addition, the results also confirm that it is appropriate to approximate/assume the costs for transmitting different packets being i.i.d. and it is appropriate to obtain

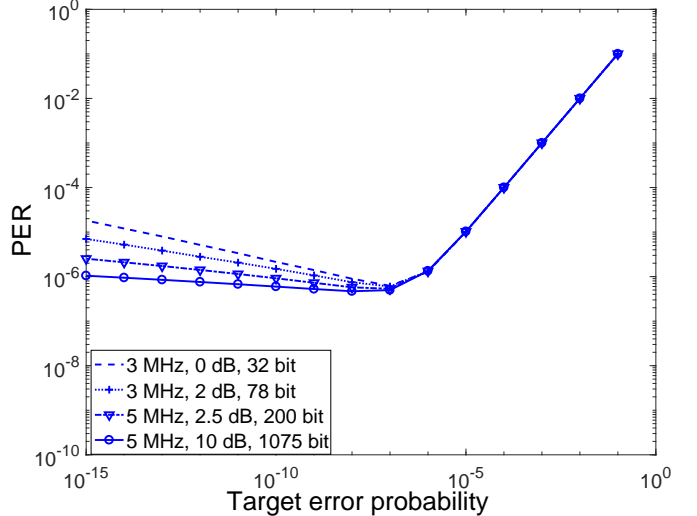


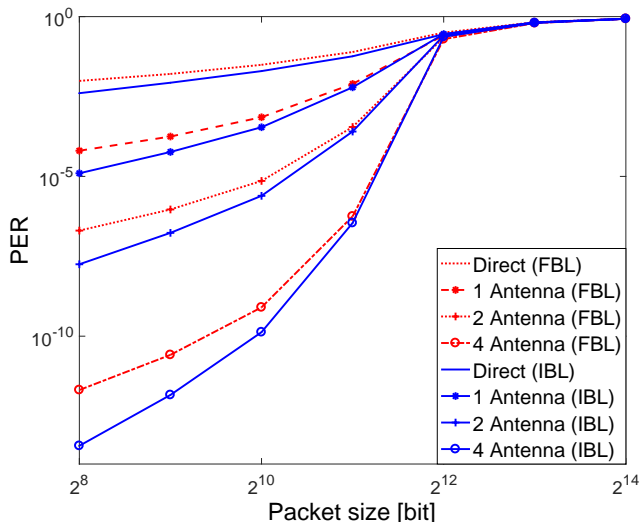
Fig. 6. PER of 4 Antenna for different channel bandwidths, SNRs, and packet sizes varying the target error probability ϵ^* .

the distribution of the blocklength cost (discrete random variable) by sampling the initially considered continuous variable. Moreover, these results together with Fig. 2 confirm Proposition 1 (cf. Sec. III-B), showing that the PER_{FBL} is convex in ϵ^* . To the left of the optimum, the system performance is dominated by scheduling errors, whereas to the right the performance is dominated by decoding errors. This is the reason for the (log-log) linear increase in the packet error rate to the right of the optimum, which can not be influenced. Once the optimum is reached, the PER_{FBL} increases moderately with a lower ϵ^* for the considered parameterization. In the following, we consider the left-hand side of the optimum in more detail.

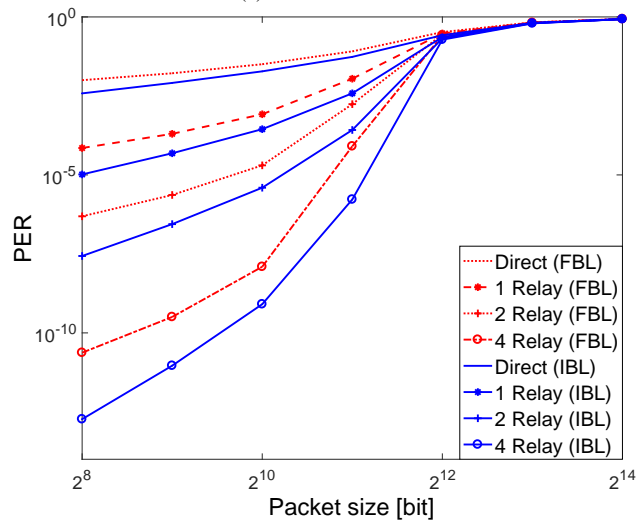
In Fig. 6, we consider BEST-ANTENNA for 4 antenna and vary the channel bandwidth, SNRs, and packet sizes. In all cases, the PER curves are convex in ϵ^* . The slope on the left side of the optimum differs depending on available bandwidth, SNR and packet size. We attribute this to the impact of the different parameters on the scheduling errors. For instance, the narrower the bandwidth, the lower is the amount of total resources for transmitting all packets, and thus the more sensitive is the scheduling error probability regarding the choice of the decoding error probability ϵ^* . This also holds for lower average SNRs obviously. The key observation though is that the slope on the right-hand side of the optimum is generally steeper than the one on the left-hand side. This implies that for practically all real system settings, a rather conservative choice of the decoding error probability ϵ^* is to be made if system parameters such as the average SNR are uncertain. The error from the choice is significantly smaller than the error from choosing a too large decoding error probability ϵ^* .

C. Finite Versus Infinite Blocklength Regime

In this section, we evaluate the proposed system in a more general way, analyzing the performance gap between FBL



(a) BEST-ANTENNA



(b) BEST-RELAY

Fig. 7. PER when varying the packet size D for BEST-ANTENNA and BEST-RELAY.

and IBL. More specifically, we investigate the PER of BEST-ANTENNA and BEST-RELAY while varying packet sizes, SNR, number of terminals, and CSI acquisition overhead based on the parametrization of Table I.

1) *Packet Size*: We begin with the packet size D , which we vary between 2^8 bit and 2^{14} bit. The results for BEST-ANTENNA and BEST-RELAY are depicted in Fig. 7 (a) and Fig. 7 (b), respectively. In general, a higher number of antennas or relays decreases the PER due to an increasing cooperative diversity. In addition, when approaching $D = 2^{12}$ bit, the PER rapidly increases for both regimes as the available transmission symbols do not suffice to reliably transmit such large packets. More interestingly, for smaller packet sizes (below 2^{10} bit), we observe a significant performance gap between the FBL and the IBL regime. This is due to the error model differences. In the IBL regime, the error is purely caused by scheduling. In the FBL regime, however, both the decoding and the scheduling error contribute to the PER_{FBL} . For small packets, the decoding error probability becomes dominant in

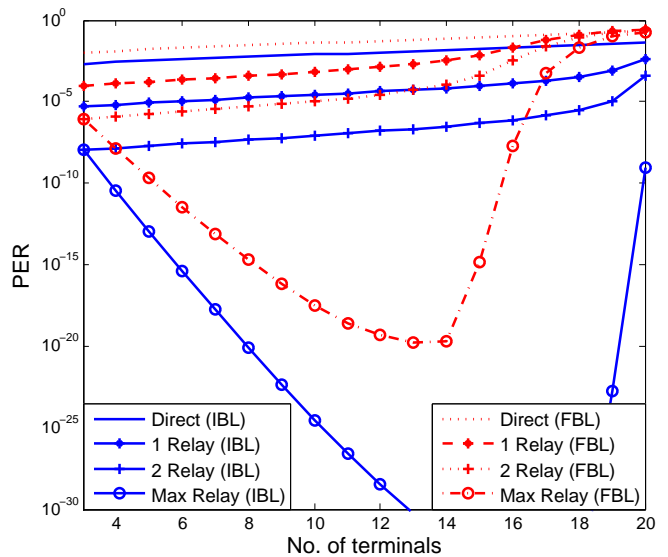


Fig. 8. The achievable PER at the optimal choice of target error probability while varying the number of terminals N for BEST-RELAY.

comparison to the scheduling error probability and essentially limits the performance. Hence, the system performance can not be arbitrarily scaled by choosing for example smaller packet sizes, which is possible for certain industrial applications. Here, an analysis performed purely on the IBL regime would be misleading. Finally, comparing the two systems we observe that BEST-ANTENNA clearly outperforms BEST-RELAY, when the number of antennas corresponds to the number of relays. This is due to a smaller overhead in case of BEST-ANTENNA as well as the performance advantage achieved through antenna switching at the base station, which was assumed with BEST-ANTENNA.

2) *Scalability*: An important question is how the performance of a cooperative system behaves with an increasing number of terminals, when considering the overhead of collecting CSI and the effects of finite blocklengths. We address this issue in Fig. 8, where we only focus on BEST-RELAY (cf. Sec. V-A). If the number of potential relay partners is limited, we observe that each additional terminal increases the achievable/minimal PER (at the optimal choice of target error probability), since the transmission resources are limited. However, if the relaying is unrestricted (we refer to this case as Max Relay) a significant performance improvement can be observed with each additional terminal as the diversity degree of the system increases. This interesting PER behavior is particularly visible under the IBL regime. However, the results under the FBL regime indicate that this behavior is not entirely accurate, especially for a higher number of terminals in the system. Although each terminal increases the diversity degree, the statistical effects of the reduced transmission symbols per terminal in combination with an increasing overhead lead to an optimal point where the reliability afterwards drastically drops. This optimal point is reached with a smaller number of terminals than the results under the IBL regime suggest.

3) *Overhead for Acquiring CSI*: Finally, we further investigate the achievable PER (at the optimal choice of the target error probability) of BEST-RELAY when using all available

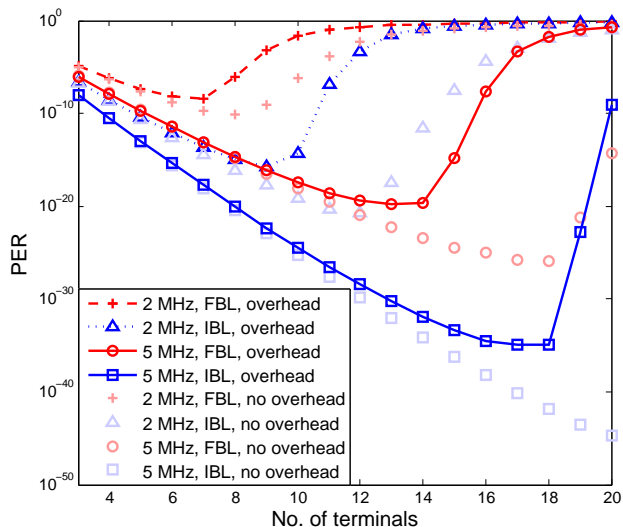


Fig. 9. The achievable PER at the optimal choice of target error probability while varying N for BEST-RELAY (Max Relay), considering different channel bandwidths B and CSI overhead assumptions.

relays (Max Relay). In Fig. 9, we consider systems with and without overhead model and vary the channel bandwidth B to illustrate their impact on the system performance. In both the IBL and the FBL regime, when an overhead model is included, the optimal PER is higher and is reached for a lower N . In addition, the gap between IBL and FBL becomes even more significant for a large bandwidth. These results again emphasize that a performance evaluation under the IBL regime compared to FBL regime is quite inaccurate and, more importantly, that the performance gap depends on different factors.

The Max Relay curves in Fig. 8 and Fig. 9 provide some insight with respect to the reliability optimization of such wireless networks. Most importantly, the results show the existence of an extremely reliable system set up, which results from the trade-off between increased system load and higher available diversity. While the absolute values are clearly subject to modeling errors stemming from abstractions, i. e., such reliability levels are likely not carrying over to reality, we emphasize that for a certain range of increasing load, the increasing diversity gain dominates the overall system performance. A subsequent question resulting from this observation is if such a behavior can be reproduced—at least qualitatively—in practical experiments.

D. Industrial Automation Scenario

Finally, we evaluate the performance of BEST-ANTENNA and BEST-RELAY in an industrial automation scenario to assess the performance of our system in a more realistic topology with heterogeneous links. After giving a detailed scenario description, we discuss the performance evaluation for both system variants.

1) *Scenario Description:* We base our evaluation topology on the Smart Automation Lab⁵, located at the Laboratory for Machine Tools and Production Engineering (WZL) of RWTH

⁵<http://www.smartautomationlab.de>

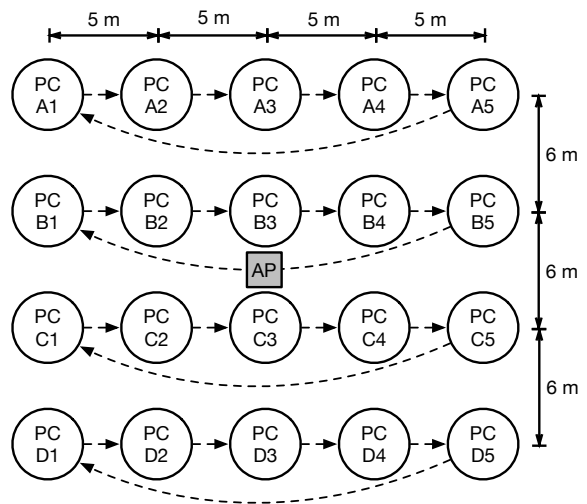


Fig. 10. Example topology for industrial automation scenario.

Aachen University. The Smart Automation Lab includes several production cells (PCs), where each PC performs a specific task in the production process and typically depends on another PC. While being wired today, wireless communication between the PCs would facilitate the modularity of the PCs and ultimately reduce costs. Thus, we consider a realistic topology with four production rows, where each row contains five PCs as shown in Fig. 10. In each production line, each PC signals to its successor that the process progress is within the expected parameters, where the last PC in a row transmits this information back to the first PC. The wireless communication is centrally managed by the AP.

For the evaluation, we use the same parameterization as listed in Table I, except that the assumption on a homogeneous average SNR for all links does not apply anymore. We set the transmit power of PCs and the AP to 0 dBm to minimize interference to co-existing wireless systems, while the noise floor is assumed to be at -80 dBm. For the path loss, we resort to an appropriate industrial model [23] with:

$$PL_{dB} = A \log_{10}(d_{[m]}) + B + X_{SF}, \quad (27)$$

where $d_{[m]}$ denotes the transmission distance in meters and X_{SF} is a lognormal-distributed variable with zero-mean and standard deviation σ_{SF} accounting for the shadow fading. [23] performed measurements at the Smart Automation Lab determining the path loss coefficients to $A = 21.75$, $B = 47.08$, and $\sigma_{SF} = 2.4$ for the 5.85 GHz band.

2) *Evaluation Results:* Based on the aforementioned scenario, we first evaluate for $N = 5$ (cf. production line B in Fig. 10) the behavior of the achievable PER when changing the target error probability ϵ^* . The results, which are shown in Fig. 11, confirm the convexity of PER_{FBL} in ϵ^* for all system variants. After reaching the optimum of 4 Antennas / Relays, the gap in the PER between the two system variants is about two orders of magnitude. This gap is more significant than in a corresponding homogeneous scenario, where the results of such a scenario are also shown for comparison purposes. This is due to the positioning of the AP in BEST-ANTENNA: Considering production line B, the AP in

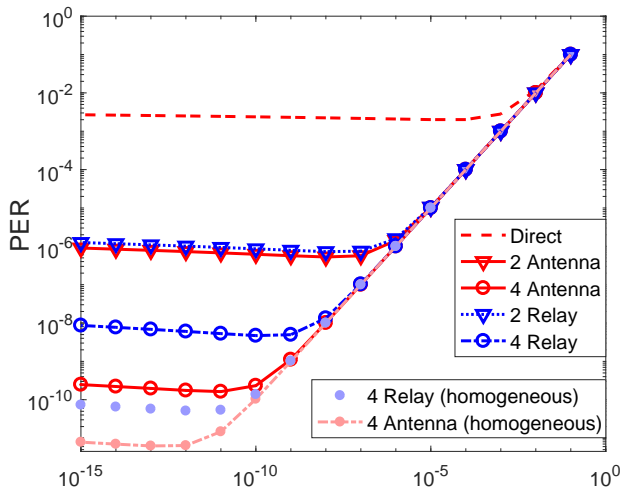


Fig. 11. PER depending on ϵ^* in the considered topology compared to the homogeneous links topology.

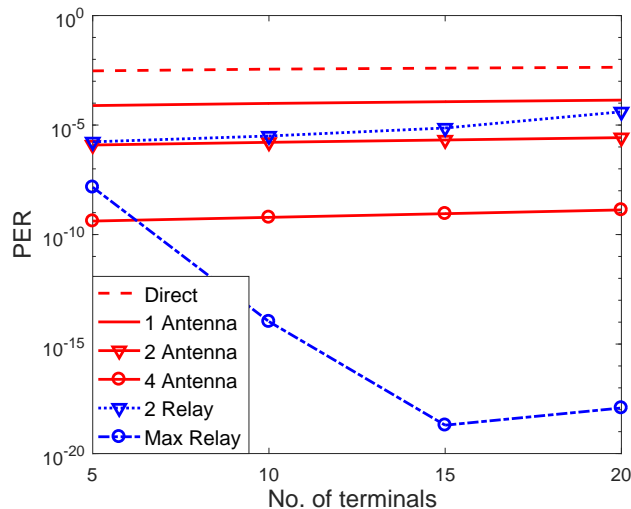


Fig. 12. The achievable PER (at the optimal choice of target error probability) of the considered industrial automation scenario.

the real deployment has on average a more central location in comparison to the potential relays and therefore BEST-ANTENNA significantly outperforms BEST-RELAY. Secondly, we evaluate the reliability for different N , i.e., we start with one production row ($N = 5$), then we add another one ($N = 10$) and so on. The respective results are depicted in Fig. 12. In both system variants, the reliability increases with the number of antennas or relays. For BEST-ANTENNA, however, we need a high degree of diversity, i.e., at least four antennas, to achieve a PER of 10^{-9} , since the direct links are in general stronger than the links to the AP, although the AP is positioned centrally. For BEST-RELAY, in turn, it is worth to apply the “Max Relay” case, at least until roughly 15 terminals. For larger topologies, the number of relays should be limited to avoid performance losses due to a large CSI overhead. In general, these results thus confirm our previous findings.

In addition, we also evaluated the performance of this industrial automation network while varying the number of hops of the cooperative communication. The results, which are not shown here, are qualitatively similar to the ones in Fig. 2 (homogeneous case), where the major performance im-

provement results from considering only 2-hop transmissions in addition to direct transmissions. Summarizing, all these results show that URLLC in industrial use cases is feasible through cooperative systems, despite the incurred overhead for CSI acquisition.

E. Extension to Rician Fading Channels

The study in previous sections under the assumption of Rayleigh fading can also be extended to the Rician fading model. The PDF of the channel fading gain of a Rician fading is given by $f_Z(z, K) = (K + 1)e^{-K-(K+1)z} \cdot I_0(2\sqrt{K(K+1)}z)$, where K is the Rician factor and $I_k(\cdot)$ is the k^{th} -order modified Bessel function of the first kind. Then, the corresponding average PER performance can be obtained based on the model in the previous sections, i.e., by substituting $f_Z(z)$ by $f_Z(z, K)$ in (20) and (21). In comparison to the Rayleigh fading model, a Rician fading channel with a line of sight (LOS) path possibly introduces a better channel quality. Hence, the expected blocklength cost (for transmitting a packet satisfying a target error probability) is decreased and the scheduling error probability and the average PER is reduced. In particular, if the fading processes of all links are also assumed to be i.i.d. (homogeneous scenario), the PDF of the expected blocklength cost is the same for all links. Therefore, in comparison to the model in the previous sections, the Rician fading introduces an equal influence on the blocklength cost for transmissions to all terminals. In particular, the impact of target error probability on the scheduling error and the average PER does not change. In the following, we provide numerical findings that support the above line of argumentation by providing a numerical investigation on the PER under a Rician fading scenario with heterogeneous links, i.e., considering the topology provided in Fig. 10. The results are shown in Fig. 13. From the figure, we observe that the PER under a Rician fading scenario is convex in the target error probability as well for different choices

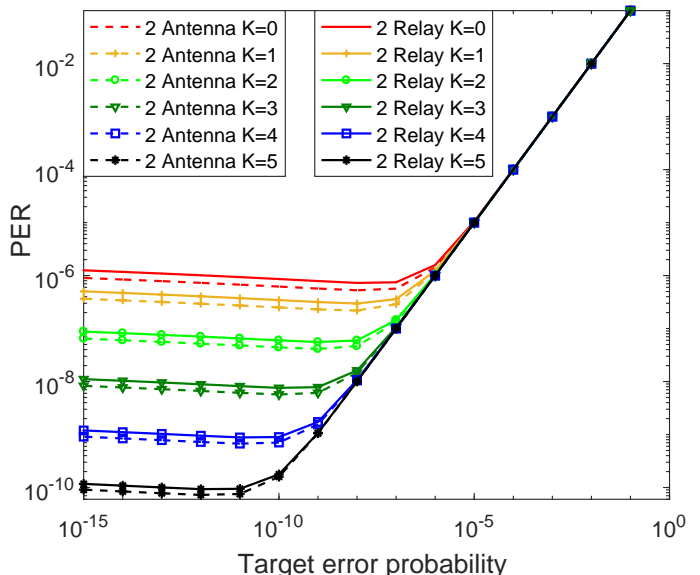


Fig. 13. PER depending on ϵ^* under a Rician fading model for the topology provided in Fig. 10.

of K , which corresponds to our findings for the Rayleigh fading scenario. Moreover, as expected, a high value of K (corresponding to a strong LOS path) results in a low PER.

F. Throughput Performance Discussion

Although the focus of this work is on the reliability performance of the considered multi-terminal networks, we conclude the numerical section with some remarks on the throughput performance to point out the general differences of these two metrics. Note that for all above studied scenarios, we have a fixed packet size of D . Hence, the corresponding (average) sum throughput over N terminals in bits per frame can be obtained by $\mu_{\text{sum}} = (1 - \text{PER}) \cdot D \cdot N$ showing that μ_{sum} is strongly influenced by the PER. Recall that we have analytically and simulatively shown that the PER is convex in the target error probability. Hence, for given D and N , μ_{sum} is concave in the target error probability. In addition, the PER is observed to be increasing in the packet size D . Note that $\mu_{\text{sum}} = (1 - \text{PER}) \cdot D \cdot N$ is decreasing with the PER but increasing with D . Hence, μ_{sum} is expected to be concave/quasi-concave in D . Moreover, under the Max Relay case we have numerically shown that the PER is quasi-convex in the number of terminals in the network N . Therefore, the throughput is expected to be concave or quasi-concave in N . Numerical studies, not shown in this paper, confirm these findings.

VI. CONCLUSION

In this work, we consider the reliability performance of multi-terminal wireless industrial networks operating based on finite blocklength codes and leveraging cooperative diversity. We primarily show that under the FBL regime the PER of the studied network is convex in the target error probability of each link. This allows for an efficient optimization of the system performance to minimize the expected packet error rate. Two factors are traded-off with respect to the optimum: On the one hand, scheduling errors arise due to a limited number of symbols available for a given frame. On the other hand, a choice for the decoding error probability needs to be done. Both these error sources influence each other, leading to an optimal choice of the decoding error probability with respect to minimizing the overall packet error probability. Numerically, we show that a cooperative system does not benefit significantly from scheduling paths with more than two hops. Furthermore, the trade-off between the scheduling and decoding errors leads in almost all cases to an optimum. Due to the nature of the optimum, we furthermore find that in almost all cases a more conservative decoding error probability should be chosen in case that system parameters are uncertain, as the gradient around the optimum implies a smaller error for lower-than-optimal choices of the decoding error probability. Analyzing the considered systems through the FBL and IBL model reveals furthermore strong performance differences which in several cases can lead to false conclusions if only considering the IBL model. Finally, when considering our investigated system models with respect to more realistic industrial scenarios with either Rayleigh or Rician fading

channels, we confirmed that cooperative systems are able to provide ultra-reliable communications at low latencies.

APPENDIX A PROOF OF PROPOSITION 1

According to Eq. (7), regarding the PER for a packet j , $j = 1, 2, \dots, N$, we have

$$\begin{aligned} \frac{\partial \text{PER}_{\text{FBL},j}}{\partial \varepsilon_{\text{ave},j}^*} &= -\frac{\partial p_j}{\partial \varepsilon_{\text{ave},j}^*} + \frac{\partial p_j}{\partial \varepsilon_{\text{ave},j}^*} \varepsilon_{\text{ave},j}^* + p_j, \\ \frac{\partial^2 \text{PER}_{\text{FBL},j}}{\partial^2 \varepsilon_{\text{ave},j}^*} &= -\frac{\partial^2 p_j}{\partial^2 \varepsilon_{\text{ave},j}^*} + \frac{\partial^2 p_j}{\partial^2 \varepsilon_{\text{ave},j}^*} \varepsilon_{\text{ave},j}^* + 2 \frac{\partial p_j}{\partial \varepsilon_{\text{ave},j}^*}. \end{aligned}$$

We first study the PER of packet 1 and subsequently, we will extend the analysis to packet j , with $j \geq 2$. According to our system model, packet 1 could be transmitted either via the direct link or using relaying. In the following, these two cases are discussed separately.

- 1) If packet 1 is transmitted via the direct link, we have $\varepsilon_{\text{ave},i}^* = \varepsilon^*$. The probability of successfully scheduling packet 1 is $p_1 = \int_{\gamma^*/\bar{\gamma}}^{+\infty} e^{-z} dz = \frac{e^{-\gamma^*/\bar{\gamma}}}{\bar{\gamma}}$ with first and second derivatives with respect to ε^* : $\frac{\partial p_1}{\partial \varepsilon^*} = -\frac{1}{\bar{\gamma}^2} \frac{\partial \gamma^*}{\partial \varepsilon^*} e^{-\gamma^*/\bar{\gamma}}$ and $\frac{\partial^2 p_1}{\partial^2 \varepsilon^*} = \frac{1}{\bar{\gamma}^2} e^{-\gamma^*/\bar{\gamma}} \left(\frac{1}{\bar{\gamma}} \left(\frac{\partial \gamma^*}{\partial \varepsilon^*} \right)^2 - \frac{\partial^2 \gamma^*}{\partial^2 \varepsilon^*} \right)$.

Therefore, we have:

$$\begin{aligned} \frac{\partial^2 \text{PER}_{\text{FBL},1}}{\partial^2 \varepsilon^*} &= 2 \frac{\partial p_1}{\partial \varepsilon^*} - (1 - \varepsilon^*) \frac{\partial^2 p_1}{\partial^2 \varepsilon^*} = \\ &= \frac{1}{\bar{\gamma}^2} e^{-\gamma^*/\bar{\gamma}} \left\{ (1 - \varepsilon^*) \left(\frac{\partial^2 \gamma^*}{\partial^2 \varepsilon^*} \varepsilon^* - \frac{1}{\bar{\gamma}} \left(\frac{\partial \gamma^*}{\partial \varepsilon^*} \right)^2 \right) - 2 \frac{\partial \gamma^*}{\partial \varepsilon^*} \right\}. \end{aligned} \quad (28)$$

Based on Eq. (15), we have

$$\dot{Q}^{-1}(\varepsilon^*) = \frac{\sqrt{M}}{\log_2 e} \frac{1 - \frac{1}{(\gamma^2 + 2\gamma)} (C_{\text{IBL}}(\gamma) - D/M)}{\sqrt{\gamma^2 + 2\gamma}} \frac{\partial \gamma^*}{\partial \varepsilon^*}.$$

According to the definition of Q-function, the first derivative of $Q^{-1}(\varepsilon^*)$ with respect to ε^* is given by

$$\dot{Q}^{-1}(\varepsilon^*) = -\sqrt{2\pi} e^{-\frac{(Q^{-1}(\varepsilon^*))^2}{2}} < 0.$$

Therefore, $1 - \frac{1}{(\gamma^2 + 2\gamma)} (C_{\text{IBL}}(\gamma) - D/M) > 0$ as $\gamma^2 + 2\gamma > \log_2(1 + \gamma) = C_{\text{IBL}}(\gamma) > C_{\text{IBL}}(\gamma) - D/M$ for $\gamma > 0$. Hence, $\frac{\partial \gamma^*}{\partial \varepsilon^*} < 0$. In particular, we have

$$\begin{aligned} \frac{\bar{\gamma}}{2} \frac{\partial \gamma^*}{\partial \varepsilon^*} &= \frac{\bar{\gamma}}{2} \frac{-\sqrt{2\pi} e^{-\frac{(Q^{-1}(\varepsilon^*))^2}{2}}}{\frac{\sqrt{M}}{\log_2 e} \frac{1 - \frac{1}{(\gamma^2 + 2\gamma)} (C_{\text{IBL}}(\gamma) - D/M)}{\sqrt{\gamma^2 + 2\gamma}}} \\ &< -\bar{\gamma} \sqrt{\frac{(\gamma^2 + 2\gamma)}{M}} \cdot e^{-\frac{M(1+\gamma)^2}{\log_2 e \sqrt{(\gamma^2 + 2\gamma)}}} \ll -1. \end{aligned}$$

Similarly, the second derivative of $Q^{-1}(\varepsilon^*)$ with respect to ε^* can be derived, based on Eq. (15) and the definition of Q -function, as

$$\begin{aligned}\ddot{Q}^{-1}(\varepsilon^*) &= \frac{\sqrt{M}}{\log_2 e} \frac{1 - \frac{1}{(\gamma^2 + 2\gamma)} (C_{\text{IBL}}(\gamma) - \frac{D}{M})}{\sqrt{\gamma^2 + 2\gamma}} \frac{\partial^2 \gamma^*}{\partial^2 \varepsilon^*} \\ &\quad - \frac{\sqrt{M}}{\log_2 e} \frac{1 - \frac{1}{(\gamma^2 + 2\gamma)} (C_{\text{IBL}}(\gamma) - \frac{D}{M})}{(\gamma^2 + 2\gamma)^{\frac{3}{2}}} \left(\frac{\partial \gamma^*}{\partial \varepsilon^*} \right)^2, \\ \ddot{Q}^{-1}(\varepsilon^*) &= 2\pi Q^{-1}(\varepsilon^*) e^{(Q^{-1}(\varepsilon^*))^2} > 0, \quad \varepsilon^* < 0.5.\end{aligned}$$

Moreover, we have $\frac{\partial^2 \gamma^*}{\partial^2 \varepsilon^*} < 0$, then

$$\frac{\partial^2 \text{PER}_{\text{FBL},1}}{\partial^2 \varepsilon^*} > \frac{1}{\bar{\gamma}^3} e^{-\gamma^*/\bar{\gamma}} \frac{\partial \gamma^*}{\partial \varepsilon^*} \left(-2 - \bar{\gamma} \frac{\partial \gamma^*}{\partial \varepsilon^*} \right) > 0,$$

as $\frac{\bar{\gamma}}{2} \frac{\partial \gamma^*}{\partial \varepsilon^*} < -1$. Hence, $\frac{\partial^2 \text{PER}_{\text{FBL},1}}{\partial^2 \varepsilon^*} > 0$ for the direct transmission case.

- 2) Packet 1 might also be transmitted via a multi-hop relaying link, i.e., a w -hop link with $w = 2, 3, 4, \dots$. Then, we have $\varepsilon_{\text{ave},i}^* = 1 - (1 - \varepsilon^*)^w \approx w\varepsilon^*$ (see Footnote 2). Hence, the PER of this packet is given by $\text{PER}_{\text{FBL},1} = 1 - p_1 + w\varepsilon^* p_1$. Note that $f_{M_{\text{hop},v},1}$ is the PDF of the blocklength cost for transmitting packet 1 via the v -th hop, $v = 1, \dots, w$. In particular, $f_{M_{\text{hop},v},1}$ has exactly the same expression as p_1 in the above direct transmission case (also the PDF of the blocklength cost via a single link). Hence, for the multi-hop case, the first and second derivatives of the PER with respect to ε^* are given by $\frac{\partial \text{PER}_{\text{FBL},1}}{\partial \varepsilon^*} = -\frac{\partial p_1}{\partial \varepsilon^*} (1 - w\varepsilon^*) + wp_1$ and

$$\begin{aligned}\frac{\partial^2 \text{PER}_{\text{FBL},1}}{\partial^2 \varepsilon^*} &= -\frac{\partial^2 p_1}{\partial^2 \varepsilon^*} (1 - w\varepsilon^*) + (\varepsilon^* + w) \frac{\partial p_1}{\partial \varepsilon^*} \\ &= -(\varepsilon^* + w) \frac{1}{\bar{\gamma}^2} \cdot \frac{\partial \gamma^*}{\partial \varepsilon^*} e^{-\gamma^*/\bar{\gamma}} \otimes f_{M_{\text{hop}2},1}(S) \otimes \\ &\quad \dots \otimes f_{M_{\text{hop}w},1}(S) \\ &\quad - (1 - w\varepsilon^*) \frac{1}{\bar{\gamma}^2} e^{-\frac{\gamma^*}{\bar{\gamma}}} \left(\frac{1}{\bar{\gamma}} \left(\frac{\partial \gamma^*}{\partial \varepsilon^*} \right)^2 - \frac{\partial^2 \gamma^*}{\partial^2 \varepsilon^*} \right) \otimes f_{M_{\text{hop}2},1}(S) \\ &\quad \dots \otimes f_{M_{\text{hop}w},1}(S) \\ &= \frac{1}{\bar{\gamma}^2} e^{-\frac{\gamma^*}{\bar{\gamma}}} \left\{ -(\varepsilon^* + w) \frac{\partial \gamma^*}{\partial \varepsilon^*} - (1 - w\varepsilon^*) \left(\frac{1}{\bar{\gamma}} \left(\frac{\partial \gamma^*}{\partial \varepsilon^*} \right)^2 - \frac{\partial^2 \gamma^*}{\partial^2 \varepsilon^*} \right) \right\} \\ &\quad \otimes f_{M_{\text{hop}2},1}(S) \dots \otimes f_{M_{\text{hop}w},1}(S) \\ &> \frac{1}{\bar{\gamma}^2} e^{-\frac{\gamma^*}{\bar{\gamma}}} \left\{ -w \frac{\partial \gamma^*}{\partial \varepsilon^*} - (1 - \varepsilon^*) \left(\frac{1}{\bar{\gamma}} \left(\frac{\partial \gamma^*}{\partial \varepsilon^*} \right)^2 - \frac{\partial^2 \gamma^*}{\partial^2 \varepsilon^*} \right) \right\} \\ &\quad \otimes f_{M_{\text{hop}2},1}(S) \dots \otimes f_{M_{\text{hop}w},1}(S) > 0,\end{aligned}$$

Note that it has been shown in 1) that $\frac{\partial \gamma^*}{\partial \varepsilon^*} < 0$ and in particular in Eq. (28) that

$$-2 \frac{\partial \gamma^*}{\partial \varepsilon^*} - (1 - \varepsilon^*) \left(\frac{1}{\bar{\gamma}} \left(\frac{\partial \gamma^*}{\partial \varepsilon^*} \right)^2 - \frac{\partial^2 \gamma^*}{\partial^2 \varepsilon^*} \right) > 0,$$

thus we have $\frac{\partial^2 \text{PER}_{\text{FBL},1}}{\partial^2 \varepsilon^*} > 0$ for the w -hop relaying case with $w \geq 2$.

So far, we have shown the convexity of the PER of packet 1 with respect to ε^* for the direct transmission and the relaying case. Note that due to random channel fading packet 1 is either transmitted directly or via a multi-hop relay. Hence, the expected PER of packet 1 is the sum of the weighted PERs of all these cases, while the weights are probabilities with non-negative values. Therefore, The $\text{PER}_{\text{FBL},1}$ is convex in ε^* .

In the following, we consider the PER of a packet j , $j \geq 2$. Recall that the source determines the transmission mode (either relaying or direct transmission) and selects the relay independently for each packet, i.e., $M_{\text{min},i}$, $i = 1, \dots, N$, are i.i.d. Note that it holds that $\frac{\partial(f(x) \otimes g(x))}{\partial x} = \frac{\partial f(x)}{\partial x} \otimes g(x)$ for the derivative of a convolution product. Hence, according to Eq. (13), we have $\frac{\partial p_i}{\partial \varepsilon^*} = \frac{\partial p_1}{\partial \varepsilon^*} \otimes f_{M_{\text{min},2}}(S) \otimes \dots \otimes f_{M_{\text{min},j}}(S)$ and

$$\begin{aligned}\frac{\partial^2 \text{PER}_{\text{FBL},2}}{\partial^2 \varepsilon^*} &= -\frac{\partial^2 p_2}{\partial^2 \varepsilon^*} + \frac{\partial^2 p_2}{\partial^2 \varepsilon^*} \varepsilon^* + 2 \frac{\partial p_2}{\partial \varepsilon^*} \\ &= (\varepsilon^* - 1) \frac{\partial^2 p_1}{\partial^2 \varepsilon^*} \otimes f_{M_{\text{min},2}}(S) \dots \otimes f_{M_{\text{min},j}}(S) \\ &\quad + 2 f_{M_{\text{min},1}}(S) \otimes f_{M_{\text{min},2}}(S) \dots \otimes f_{M_{\text{min},j}}(S) \\ &= \left(\frac{\partial^2 p_1}{\partial^2 \varepsilon^*} (\varepsilon^* - 1) + 2 \frac{\partial p_1}{\partial \varepsilon^*} \right) \otimes f_{M_{\text{min},2}}(S) \dots \\ &\quad \otimes f_{M_{\text{min},j}}(S) > 0.\end{aligned}$$

Hence, the $\text{PER}_{\text{FBL},j}$ is convex in ε^* for $j = 1, 2, \dots, N$. As the sum of convex functions is also convex, $\text{PER}_{\text{FBL}} = \frac{1}{N} \sum_{j=1}^N \text{PER}_{\text{FBL},j}$ is convex in ε^* .

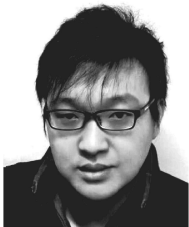
ACKNOWLEDGMENT

The research leading to these results has received funding from the German Federal Ministry of Education and Research (BMBF) within the project 16KIS0196 (KoI).

REFERENCES

- [1] J. G. Andrews, S. Buzzi, W. Choi, *et al.*, "What will 5G be?" *IEEE J. Sel. Areas Commun.*, vol. 32, no. 6, pp. 1065–1082, June 2014.
- [2] A. Frotzschner, U. Wetzker, M. Bauer *et al.*, "Requirements and current solutions of wireless communication in industrial automation," in *IEEE Int. Conf. on Comm. Workshops (ICC)*, Sydney, Australia, June 2014, pp. 67–72.
- [3] P. Neumann, "Communication in industrial automation—what is going on?" *Control Engin. Practice*, vol. 15, no. 11, pp. 1332–1347, 2007.
- [4] S. N. Diggavi, N. Al-Dhahir, A. Stamoulis, and A. R. Calderbank, "Great expectations: The value of spatial diversity in wireless networks," *Proceedings of the IEEE*, vol. 92, no. 2, pp. 219–270, Feb. 2004.
- [5] J. N. Laneman, D. N. C. Tse, and G. W. Wornell, "Cooperative diversity in wireless networks: Efficient protocols and outage behavior," *IEEE Trans. on Inform. Theory*, vol. 50, no. 12, pp. 3062–3080, Dec. 2004.
- [6] A. Bletsas, A. Khisti, D. P. Reed, and A. Lippman, "A Simple cooperative diversity method based on network path selection," *IEEE J. Sel. Areas Commun.* vol. 24, no. 3, pp. 659–672, Mar. 2006.
- [7] A. Bletsas and A. Lippman, "Implementing cooperative diversity antenna arrays with commodity hardware," *IEEE Commun. Mag.*, vol. 44, no. 12, pp. 33–40, Dec. 2006.
- [8] A. Chaaban and A. Sezgin, "Multi-Hop Relaying: An end-to-end delay analysis," *IEEE Trans. on Wireless Comm.*, vol. 15, no. 4, pp. 2552–2561, Apr. 2016.
- [9] V. N. Swamy, S. Suri, P. Rigge *et al.*, "Cooperative communication for high-reliability low-latency wireless control," in *IEEE Int. Conf. on Comm. (ICC)*, London, UK, June 2015, pp. 4380–4386.
- [10] C. Dombrowski and J. Gross, "EchoRing: A low-latency, reliable token-passing MAC protocol for wireless industrial networks," in *Proc. of 21th European Wireless Conference (EW15)*, Budapest, Hungary, May 2015.
- [11] M. Serror, C. Dombrowski, K. Wehrle, and J. Gross, "Channel coding versus cooperative ARQ: Reducing outage probability in ultra-low latency wireless communications," in *IEEE Global Comm. Conf. (GLOBECOM) Workshops (ULTRA²)*, San Diego, USA, Dec. 2015.
- [12] Y. Polyanskiy, H. Poor, and S. Verdú, "Channel coding rate in the finite blocklength regime," *IEEE Trans. on Inform. Theory*, vol. 56, no. 5, pp. 2307–2359, 2010.
- [13] Y. Hu, J. Gross, and A. Schmeink, "On the capacity of relaying with finite blocklength," *IEEE Trans. Veh. Technol.*, vol. 62, no. 5, pp. 1490–1502, Mar. 2015.

- [14] Y. Hu, J. Gross, and A. Schmeink, "On the performance advantage of relaying under the finite blocklength regime," *IEEE Comm. Letter*, vol. 62, no. 5, pp. 1490–1502, July 2015.
- [15] Y. Hu, M. C. Gursoy and A. Schmeink, "Relaying-enabled ultra-reliable low latency communications in 5G", *IEEE Network*, accepted to appear.
- [16] Y. Hu, J. Gross, and A. Schmeink, "Blocklength-limited performance of relaying under quasi-static Rayleigh channels," *IEEE Trans. on Wireless Comm.*, vol. 15, no. 7, pp. 4548–4558, July 2016.
- [17] Y. Wei, G. Durisi, T. Koch, and Y. Polyanskiy, "Quasi-static multiple-antenna fading channels at finite blocklength," *IEEE Trans. on Inform. Theory*, vol. 60, no. 7, pp. 4232–4265, July 2014.
- [18] S. Xu, T. H. Chang, S. C. Lin *et al.*, "Energy-efficient packet scheduling with finite blocklength codes: Convexity analysis and efficient algorithms," *IEEE Trans. on Wireless Comm.*, vol. 15, no. 8, pp. 5527–5540, Aug. 2016.
- [19] G. Ozcan and M. C. Gursoy, "Throughput of cognitive radio systems with finite blocklength codes," *IEEE J. Sel. Areas Commun.* vol. 31, no. 11, pp. 2541–2554, Nov. 2013.
- [20] B. Makki, T. Svensson, and M. Zorzi, "Finite block-length analysis of the incremental redundancy HARQ," *IEEE Wireless Comm. Letters*, vol. 3, no. 5, pp. 529–532, Oct. 2014.
- [21] B. Makki, T. Svensson, and M. Zorzi, "Finite block-length analysis of spectrum sharing networks using rate adaptation," *IEEE Trans. on Comm.*, vol. 63, no. 8, pp. 2823–2835, Aug. 2015.
- [22] Y. Polyanskiy, H. V. Poor, and S. Verdú, "Dispersion of the Gilbert-Elliott Channel," *IEEE Trans. Veh. Technol.*, vol. 57, no. 4, pp. 1829–1848, Apr. 2011.
- [23] B. Holfeld, D. Wieruch, L. Raschkowsk *et al.* "Radio channel characterization at 5.85 GHz for wireless M2M communication of industrial robots," in *IEEE Wireless Communications and Networking Conference*, Doha, Qatar, Apr. 2016.



Yulin Hu received his M.Sc.E.E degree from USTC, China, in 2011. He successfully defended his dissertation of a joint Ph.D. program supervised by Prof. Anke Schmeink at RWTH Aachen University and Prof. James Gross at KTH Royal Institute of Technology in Dec. 2015 and received his Ph.D.E.E. degree (with honors) from RWTH Aachen University where he is a Research Fellow since 2016. From May to July in 2017, he was a visiting scholar with Prof. M. Cenk Gursoy in Syracuse University, USA.

His research interests are in information theory, optimal design of wireless communication systems. He has been invited to contribute submissions to multiple conferences. He received the Best Paper Awards at IEEE ISWCS 2017 and IEEE PIMRC 2017, respectively. He is currently serving as an editor for Physical Communication (Elsevier).



Martin Serror received the B.Sc. degree in computer science at RWTH Aachen University in 2012. Afterwards, he studied abroad at Universitat Politècnica de València, Spain, for two semesters. He returned to RWTH Aachen University and obtained the M.Sc. degree in computer science in 2014 (with honors). Currently, he is working toward the Ph.D. degree at the Chair of Communication and Distributed Systems (COMSYS). His research interests lie mainly in the design and the performance evaluation of communication protocols for critical

machine-to-machine communications and dependable wireless systems. He received the Best Demo Award at IEEE WoWMoM 2015 and the Best Paper Award at IEEE LCN 2015.



Klaus Wehrle received the Diploma (equiv. M.Sc.) and Ph.D. degrees from University of Karlsruhe (now KIT), both with honors. He is full professor of Computer Science and Head of the Chair of Communication and Distributed Systems (COMSYS) at RWTH Aachen University. His research interests include (but are not limited to) engineering of networking protocols, (formal) methods for protocol engineering and network analysis, reliable communication software, as well as all operating system issues of networking. He was awarded Junior

Researcher of the Year (2007) by the German Association of Professors (Deutscher Hochschulverband). He is member of IEEE, ACM, SIGCOMM, GI (German Informatics Society), VDE, GI/ITG-Fachgruppe KuVS, the main scholarship board of Humboldt Foundation, the Scientific Directorate of Dagstuhl, and the German National Academy of Science and Engineering (ACATECH).



James Gross received his Ph.D. degree from TU Berlin in 2006. From 2008-2012 he was Assistant Professor and Head of the Mobile Network Performance Group at RWTH Aachen University, as well as a member of the DFG-funded UMIC Research Centre of RWTH. Since November 2012, he has been with the School of Electrical Engineering and Computer Science, KTH Royal Institute of Technology, Stockholm, as an Associate Professor. He also serves as Director for the ACCESS Linneaus Centre and is a board member of KTHs Innovative

Centre for Embedded Systems. His research interests are in the area of mobile systems and networks, with a focus on critical machine-to-machine communications, cellular networks, resource allocation, as well as performance evaluation methods. He has authored over 100 (peer-reviewed) papers in international journals and conferences. His work has been awarded multiple times, including best paper awards at ACM MSWiM 2015, the Best Demo Paper Award at IEEE WoWMoM 2015, the Best Paper Award at IEEE WoWMoM 2009, and the Best Paper Award at European Wireless 2009. In 2007, he was the recipient of the ITG/KuVS dissertation award for his Ph.D. thesis. He is also co-founder of R3 Communications GmbH, a Berlin-based start-up in the area of ultra-reliable low-latency wireless networks for industrial automation.